Orientation of the Temporal Nerve Fiber Raphe in Healthy and in Glaucomatous Eyes

Phillip Bedggood,[1] Bao Nguyen,[1] Graham Lakkis,[1] Andrew Turpin,[2] and Allison M. McKendrick[1]

[1]Department of Optometry & Vision Sciences, The University of Melbourne, Australia
[2]Department of Computing and Information Systems, The University of Melbourne, Australia

Correspondence: Allison M. McKendrick, Department of Optometry and Vision Sciences, Level 4 Alice Hoy Building, The University of Melbourne, Parkville, VIC 3010, Australia;
allisonm@unimelb.edu.au.

Submitted: April 4, 2017
Accepted: July 4, 2017

Citation: Bedggood P, Nguyen B, Lakkis G, Turpin A, McKendrick AM. Orientation of the temporal nerve fiber raphe in healthy and in glaucomatous eyes. *Invest Ophthalmol Vis Sci*. 2017;58:4211–4217. DOI: 10.1167/iovs.17-21995

Purpose. To determine the normal variation in orientation of the temporal nerve fiber raphe, and the accuracy with which it may be predicted or approximated in lieu of direct measurement.

Methods. We previously described an algorithm for automatic measurement of raphe orientation from optical coherence tomography, using the intensity of vertically oriented macular cubes. Here this method was applied in 49 healthy participants (age 19–81 years) and 51 participants with primary open angle glaucoma (age 51–80 years).

Results. Mean fovea-disc-raphe angle was 173.5° ± 3.2° (range = 166°–182°) and 174.2° ± 3.4° (range = 166°–184°) in healthy and glaucoma patients, respectively. Differences between groups were not significant. Fovea-disc-raphe angle was not correlated with age or axial length ($P > 0.4$), showed some symmetry between eyes in glaucoma ($R^2 = 0.31$, $P < 0.001$), and little symmetry in the healthy group ($P = 0.06$). Fovea-disc angle was correlated with fovea-raphe angle ($R^2 = 0.27$, $P = 0.0001$), but was not a good predictor for raphe orientation (average error = 6.8°). The horizontal axis was a better predictor (average error = 3.2°; maximum error = 9.6°), but still gave approximately twice the error previously reported for direct measurement from macular cubes.

Conclusions. There is substantial natural variation in temporal nerve fiber raphe orientation, which cannot be predicted from age, axial length, relative geometry of the disc and fovea, or the contralateral eye. For applications to which the orientation of the raphe is considered important, it should be measured directly.

Keywords: glaucoma, optic nerve head, perimetry, structure–function, visual field

In general, retinal nerve fibers trace either a superior or an inferior path from their site of origin to the optic nerve head. The line demarcating these two groups of fibers is known as the nerve fiber raphe.[1] In recent years it has become possible to visualize the orientation of the raphe using modern imaging methods. High resolution techniques, such as optical coherence tomography (OCT)[2] (see also Tanabe F, et al. *IOVS* 2014;55:ARVO E-Abstract 957) or adaptive optics,[3,4] allow direct visualization of individual nerve fiber bundles. Such imaging has revealed that the temporal raphe can deviate markedly from the horizontal meridian and shows substantial variability between individuals.

The temporal raphe is of particular interest in glaucoma due to characteristic losses of sensitivity in the nasal visual field.[5,6] At present, the temporal raphe is not directly measured hence clinical analysis tools make assumptions regarding the raphe position. For example, the temporal raphe is traditionally assumed to divide the visual field horizontally in order to calculate visual field metrics, such as the Glaucoma Hemifield Test[7] or Cluster Analysis.[8] In some OCT protocols, the axis of symmetry is instead assumed to be parallel to the line between the fovea and the center of the optic nerve head.[9] The potential for pronounced variations in orientation of the raphe, noted above, suggests that a given point in the nasal visual field for one patient could correspond to the opposite pole of the optic disc as the same point for another patient. This limits the extent to which data from visual field testing and anatomical assessment of the retinal nerve fiber layer can be mapped onto one another in the nasal visual field in the absence of measuring the raphe. Yet, most existing models for mapping structure to visual function presume a horizontally oriented raphe.[10,11]

Previous work incorporating high-resolution imaging to measure the orientation of the temporal raphe has only been applied to small samples of individuals, presumably because the methods require excellent fixation for long periods. Utilizing more standard, clinical imaging protocols, several studies have reported estimates of the temporal raphe position from OCT thickness measures.[5,12,13] However, the reliability of thickness-based estimates may be less than for intensity-based estimates.[14]

We recently developed a method to measure the orientation of the temporal raphe, from OCT intensity data acquired by vertically oriented macular cubes.[14] Here this method was used to measure raphe orientation in a population of 49 healthy patients and 51 patients with glaucoma. These measurements were used to determine the following:

1. The range of natural variation in raphe orientation, and symmetry between eyes.
2. Whether reductions in nerve fiber density with glaucoma, increasing age, or increasing axial length manifest as a change in apparent raphe orientation. This would be expected if nerve fiber density is reduced asymmetrically across hemifields, a phenomenon that would also be

Table. Summary of Relevant Parameters for Both Participant Groups, Given as Mean ± Standard Deviation (Range)

Group	*n*	Age, y	Refraction, D	Axial Length, mm	MD, dB
Healthy	49	51 ± 19 (19 to 81)	0.1 ± 1.3 (−3.50 to +3.75)	23.0 ± 0.9 (21.1 to 25.5)	−0.4 ± 1.3 (−4.1 to +2.4)
Glaucoma	51	70 ± 7 (51 to 80)	0.2 ± 2.0 (−6.50 to +3.50)	23.3 ± 1.1 (21.2 to 26.5)	−3.2 ± 4.2 (−14.5 to +1.4)

Refraction is given as spherical equivalent.

expected to change the local packing density of fibers as they enter the optic nerve head.

3. The extent to which raphe orientation may be predicted from commonly used assumptions, that is, that the temporal raphe is horizontal or that it is parallel to the fovea-disc axis.

Methods

Participants

Clinically acquired OCT data were retrospectively examined from both eyes of 60 healthy participants and 64 participants with glaucoma. For statistical purposes, data are reported only from the right eye of each participant, except when comparing raphe orientation between eyes. Scans suffering from excessive reflective artifact at the level of the nerve fiber layer were rejected as outlined below, resulting in a final sample of right eyes of 49 healthy participants (age 51 ± 19 years; range 19–81 years) and 51 with glaucoma (age 70 ± 7 years; range 51–80 years).

Participants undertook a comprehensive eye examination to ensure the following inclusion criteria were met: best corrected visual acuity of 6/9.5 or better, spherical refractive error between −10 diopters (D) and +6 D, astigmatism no greater than −2 D, and no ocular pathology (other than glaucoma) or surgery (apart from uncomplicated cataract surgery). Participants in the healthy group had intraocular pressure < 21 mm Hg by applanation tonometry. Participants in the glaucoma group had an ophthalmological diagnosis of open-angle glaucoma, were treated at the time of testing, and also showed structural parameters that fell outside normal limits (one-tailed 95% range of the normative database for thickness of the peripapillary retinal nerve fiber layer or minimum rim width at the opening of Bruch's membrane) on spectral domain OCT optic nerve head imaging with the Heidelberg Spectralis Glaucoma Module (Heidelberg Engineering GmBH, Germany). All glaucoma patients underwent testing with 24-2 Humphrey Field Analyzer SITA Standard visual fields and were required to have no more than 25% fixation loss and 20% false-positive rate. In the patient group, mean defect (MD) ranged from −14.5 dB to +1.4 dB; 23 patients (45%) had MD better than −2 dB; 19 (37%) had MD between −2 and −10 dB, and 5 (10%) had MD worse than −10 dB. Axial length was measured using A-scan ultrasound biometry (Tomey AL-100; Nishi-Ku, Nagoya, Japan), with the final estimate being the average of at least three repeated measures per eye.

All participants provided written informed consent prior to participation in accordance with a protocol approved by the Human Research Ethics Committee of the University of Melbourne and compliant with the tenets of the Declaration of Helsinki.

Relevant parameters for both healthy participants and those with glaucoma are summarized in the Table.

Angles of Interest

Figure 1 shows an example fundus image overlaid with OCT data from the temporal raphe, and provides definitions for the angles referred to in this paper: the fovea-disc ("FoDi"), fovea-raphe ("FoRaph"), and fovea-disc-raphe ("FoDiRaph") angles. The figure also illustrates the assumption of a horizontal raphe[5,12,13,15] (black); a continuation of the fovea-disc axis[2] (blue); and direct measurement from macular cube data[14] (magenta). Other approximations include the population mean, or a linear model based on parameters, such as FoDi angle, axial length, and age (not illustrated).

The primary outcome measure was the FoDiRaph angle. Typical head rotation between scans leads to small (±1°) differences in retinal orientation,[16] and the device/table itself should not be presumed exactly horizontal (a 2°-inclination was measured in the relevant meridian; i.e., right eye (RE) > left eye (LE). To circumvent these issues, raphe orientation is expressed by the rotation-independent angle between the fovea, disc, and raphe (FoDiRaph). FoDi and FoRaph angles are also reported where appropriate for comparison with other work.

To match the sign convention used in the Spectralis software, and as shown in Figure 1, negative FoDi angles indicate a disc that is higher than the fovea (by far the most common arrangement), and positive FoRaph angles indicate a raphe that points downward as it extends away from the fovea (also the most common example; raphes of negative sign do occur, however, as illustrated in Fig. 1).

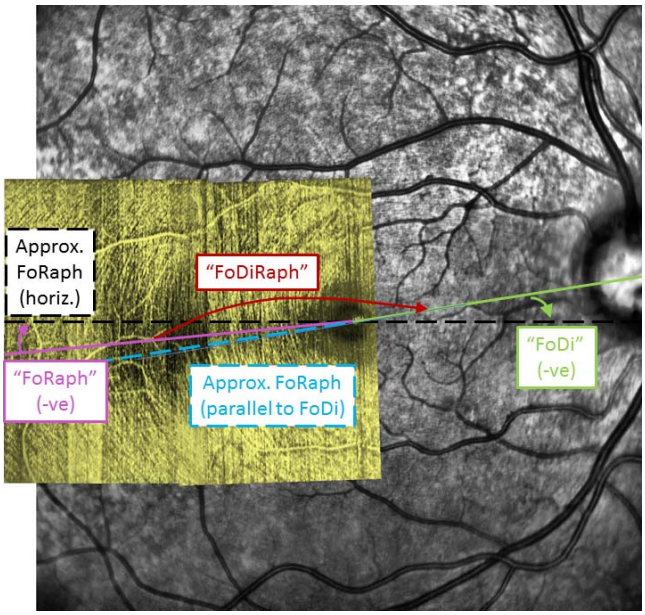

Figure 1. Definition of angles discussed in this paper, as well as candidate approximations for the fovea-disc-raphe angle. FoDi = angle between foveal center, optic disc (Bruch's membrane opening), and horizontal axis; FoRaph = angle between fovea, horizontal axis, and the measured raphe axis; FoDiRaph = angle between foveal center, optic disc, and raphe axis. Potential approximations in lieu of measuring the raphe include assuming that it is horizontal (*black dashed line*), or that it is parallel to the fovea-disc axis (*blue dashed line*). According to the sign convention adopted in this paper, in this example the FoDi and FoRaph angles are negative in sign.

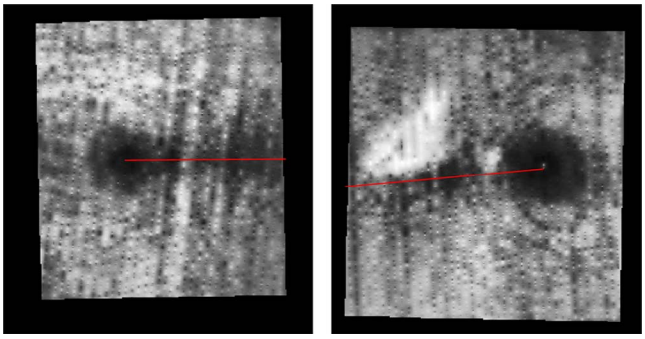

FIGURE 2. Example en face intensity images at the level of the nerve fiber, synthesized from macular cube data. *Left*: A normal image in which the dark patch corresponding to the temporal raphe is readily identifiable (*red line*: automatic determination of fovea-raphe axis). *Right*: An image rated manually as having "severe" back-reflection overlying the raphe (*red line*: attempt to automatically locate the fovea-raphe axis, which is likely in error due to the reflection).

Determination of FoDi Axis

Prior to acquisition of macular cube data, a scan pattern comprised of 24 radially oriented B-scans, 15° in diameter, was centered on the disc. The foveal pit was then manually localized using a live B-scan, as were the two boundary points of Bruch's membrane opening evident on each of two perpendicular B-scans. The labeled points were used to determine the FoDi orientation, to which subsequent macular cubes were aligned by registering the fundus images that are acquired by scanning laser ophthalmoscopy immediately prior to acquisition of each volume.

Macular Cube Acquisition

After acquisition of the disc volume, a macular cube of standard density (49 B-scans encompassing a 20°-square patch of retina) was acquired with B-scans oriented perpendicularly to the FoDi axis; that is, nominally vertical. Each B-scan was the average of 10 individual scans. Eyes that produced scans with signal strength below 20 dB were excluded from analysis. We have shown previously that visualization of the temporal nerve fiber raphe is improved by the use of vertically as opposed to horizontally oriented B-scans, due to reduction of eye movement-related artifacts, which are detrimental to localization of the temporal raphe.[14] The cube was centered approximately 3° temporally to allow more of the temporal raphe to be visualized than if the scan was centered on fixation.

After automatic segmentation of the retinal layers by the device, data were exported from the Heidelberg Eye Explorer software version 6.3, in .vol format. These data were imported to Matlab R2015b (The MathWorks, Natick, MA, USA) and processed using custom software. Our prior work had shown that intensity of the macular cube data provides a more robust estimate of raphe orientation than does thickness[14]; an en face intensity image was therefore generated at the level of the nerve fiber layer. From this image, the raphe orientation was determined as described below.

Exclusion of Data Featuring Excessive Back-Reflections

We previously reported that at the level of the nerve fiber layer, large back-reflections (Fig. 2) often arise, which substantially interfere with estimates of the raphe angle.[14] These can be avoided by purposeful misalignment of the instrument prior to image capture; however, this was not undertaken here since

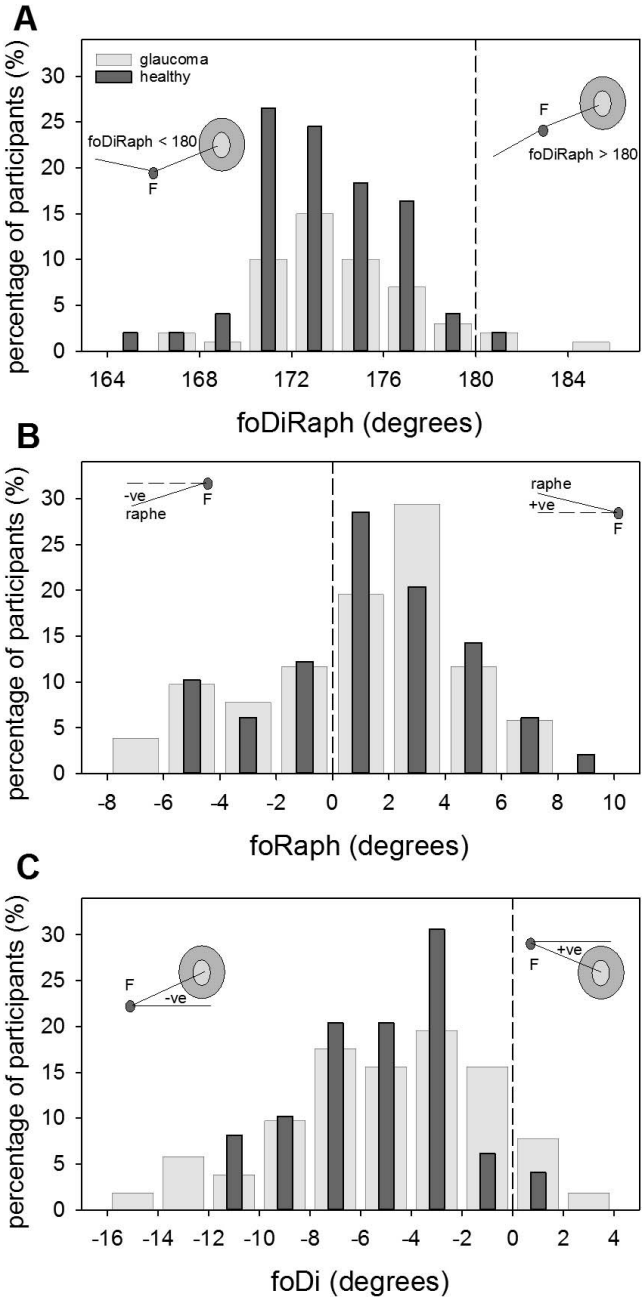

FIGURE 3. Population distribution of (**A**) the FoDiRaph angle, (**B**) FoRaph angle, and (**C**) FoDi angle. *Dark bars* show data for healthy subjects, and *light bars* for patients with glaucoma. *Inset cartoons* show examples of the sign convention for each parameter.

data were reviewed retrospectively. Instead, images were manually triaged images as having minimal, moderate, or severe back-reflections at the level of the nerve fiber layer.[14] Figure 2 shows examples of minimal (left—accepted) and severe (right—rejected) image artifacts. As mentioned above, 11 of 60 healthy participants and 13 of 64 glaucoma participants were excluded in this way, leaving $n = 49$ and $n = 51$ participants in the healthy and glaucoma groups, respectively.

Localization of the Temporal Raphe

Raphe orientation can be specified relative to the horizontal meridian (FoRaph in Fig. 1) or by the angle formed between the fovea, disc, and temporal raphe (FoDiRaph in Fig. 1). As

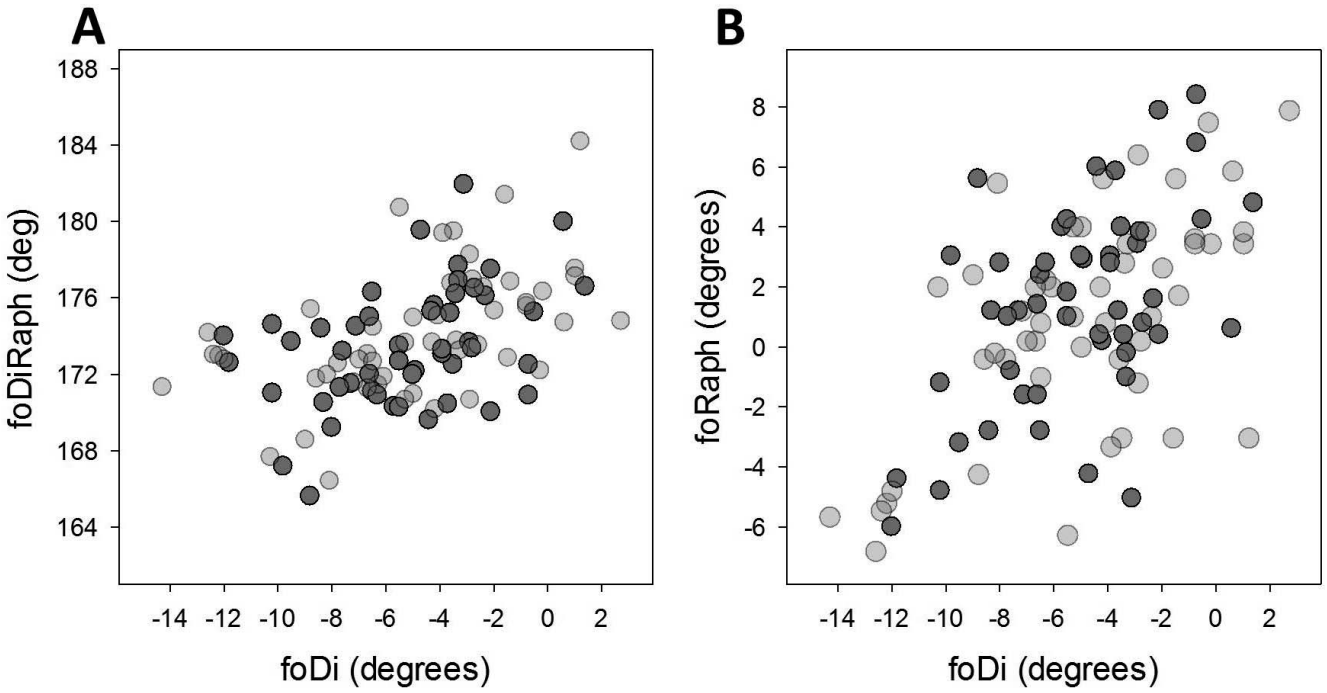

FIGURE 4. Orientation of the temporal raphe as a function of fovea-disc angle, expressed as (**A**) the angle between the fovea, disc, and raphe; (**B**) the angle between the fovea, disc, and horizontal axis. *Dark symbols* indicate healthy controls and *light symbols* indicate patients with glaucoma.

mentioned above, the latter was predominantly used here since it is more robust to rotational errors,[16] but the former is also included to give a better impression of where the raphe lies relative to horizontal.

To robustly assess both normal and glaucomatous raphes, the "med" (median) algorithm characterized in our previous work was used.[14] In brief, this algorithm operates as follows:

1. Source points are positioned on a vertical line through the foveal center.
2. From each source point, a fan of lines is traced. The line with lowest average intensity is recorded for that source point.
3. The median angle made by the source-point lines identified in step 2 is taken as the raphe.

Although we previously obtained marginally lower error (1.55°) for healthy eyes using a different algorithm,[14] when that algorithm was applied here to the glaucoma group an outlier was identified whose proposed raphe orientation did not subjectively match the en face OCT image. By applying the "med" algorithm instead, the proposed raphe orientation for all participants was subjectively well-aligned with the subjectively visualized raphe. Thus, the "med" algorithm may be more robust in atypical cases, which is important given recent suggestions that the shape of the raphe is altered in glaucoma due to erosion of the nerve fiber layer.[4]

Statistical Analysis

Statistical comparisons were made using standard functions in the Statistics and Machine Learning Toolbox of Matlab R2015b (The MathWorks). Group means were compared with a two-tailed *t*-test; Pearson correlation between variables was assessed following linear regression by least squares. Case resampling bootstrap with replacement (n = 10,000) was employed to test for differences in distribution; that is, variance, skewness, or kurtosis. Unless otherwise specified, data represent the right eye of each patient.

RESULTS

Variation in the Position of the Temporal Raphe

The mean angle defined by the anatomical locations of the fovea, disc, and raphe (FoDiRaph) was 173.5° ± 3.2° (range 166°–182°) in the healthy control eyes (Fig. 3A, dark bars). The same angle was 174.2° ± 3.4° (range 166°–184°) in the glaucoma eyes (Fig. 3A, light bars). The difference in group means was not significant [$t(98) = 1.1$, $P = 0.28$], nor were any differences in shape of the distribution statistically significant (i.e., variance, skewness, kurtosis, or Shapiro-Wilk normality score) as determined by case resampling bootstrap ($n = 10{,}000$; $P > 0.27$).

Raphe orientation can also be expressed relative to the horizontal meridian (FoRaph in Fig. 1). FoRaph was +1.3° ± 3.4° in the healthy control eyes (Fig. 3B, dark bars) and +0.9° ± 3.7° in the glaucoma eyes (Fig. 3B, light bars). The difference between groups was not significant [$t(98) = 0.6$, $P = 0.58$]. For reference, the fovea-disc angle (FoDi in Fig. 1) was −5.2 ± 3.1° (range = −12° to +1.4°) in the healthy eyes (Fig. 3C, dark bars) and −4.9° ± 4.0° (range = −14.3° to +2.7°) in the glaucoma eyes (Fig. 3C, light bars).

Relationship Between Temporal Raphe Position and Other Measures

In addition to glaucoma status, this study assessed the impact of fovea-disc orientation, the raphe orientation of the contralateral eye, age, and axial length on the orientation of the raphe.

Figure 4A plots the raphe orientation (FoDiRaph) for each patient as a function of FoDi orientation, for healthy individuals (dark symbols) and glaucoma patients (light symbols). The FoDiRaph angle was correlated with the FoDi angle in both groups ($R^2 = 0.18$ and $P = 0.002$; $R^2 = 0.27$ and $P = 0.0001$, respectively). Regression slopes were ~0.4 in both groups (95% confidence interval [CI]: 0.2–0.7). A slope significantly

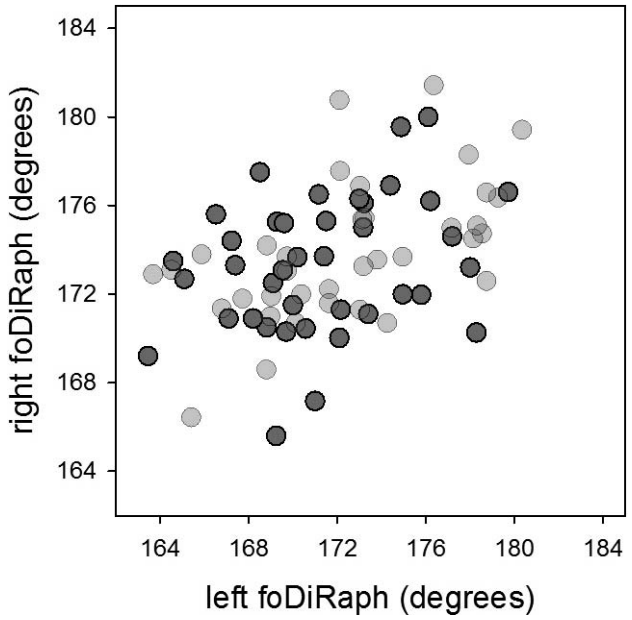

FIGURE 5. Orientation of the temporal raphe, expressed as the angle between the fovea, disc, and raphe, in the right eye as a function of that in the left eye. *Dark symbols* indicate healthy controls, and *light symbols* indicate patients with glaucoma.

less than unity suggests that the FoRaph angle must vary with the FoDi angle. These parameters are plotted against each other in Figure 4B, with linear regression confirming their association (in healthy eyes: $R^2 = 0.27$, $P = 0.0001$, slope = +0.57; in glaucoma: $R^2 = 0.36$, $P < 10^{-5}$, slope = +0.56). The sign of the regression in this case indicates that higher insertion of the disc in the globe (i.e., a more negative FoDi angle) is associated with a lower orientation of the temporal raphe (i.e., a more negative FoRaph angle); the fact that the slope is less than unity indicates that the associated raphe displacement is less than that of the disc.

Figure 5 plots the FoDiRaph angle for right eyes as a function of that for left eyes, for healthy individuals (dark symbols) and for glaucoma patients (light symbols). There was moderate enantiomorphism between eyes in the glaucoma group ($R^2 = 0.31$ and $P < 0.001$), and some trend toward enantiomorphism in the healthy group ($P = 0.06$). Interestingly, neither the fovea-disc nor the fovea-raphe angles themselves (which are used to calculate the fovea-disc-raphe angle) were correlated between eyes, for either group ($P > 0.35$).

Figure 6A plots the fovea-disc-raphe angle for the healthy participants as a function of age, showing no significant correlation ($P = 0.9$). Similarly, there was no correlation between fovea-disc-raphe angle and axial length ($P = 0.4$), as plotted in Figure 6B. Neither was there any significant correlation between these parameters in the glaucoma group (not shown), although it should be noted that the range of ages and axial lengths in this group was reduced.

Assessing the Accuracy of Various Approximations to Raphe Orientation

Figure 7A plots the absolute error for the approximations to raphe orientation, relative to the measured raphe. Boxes represent the interquartile range, whiskers the 90% range, and outliers are plotted as additional points. Because the mean accuracy of the raphe measurement method ("med") was 1.59° in our previous work, this value is plotted as well for comparison (dashed line). It should be noted that this value was derived from healthy eyes only, as the determination of accuracy requires long (10 minutes) high-resolution scans, which require excellent fixation and relatively clear optical media.[14] Nonetheless it is likely that accuracy is similar in the glaucoma population, given analysis presented below in which the uncertainty in localization of the raphe is considered.

The most error-prone approximation was to assume that the raphe is a continuation of the fovea-disc axis (average

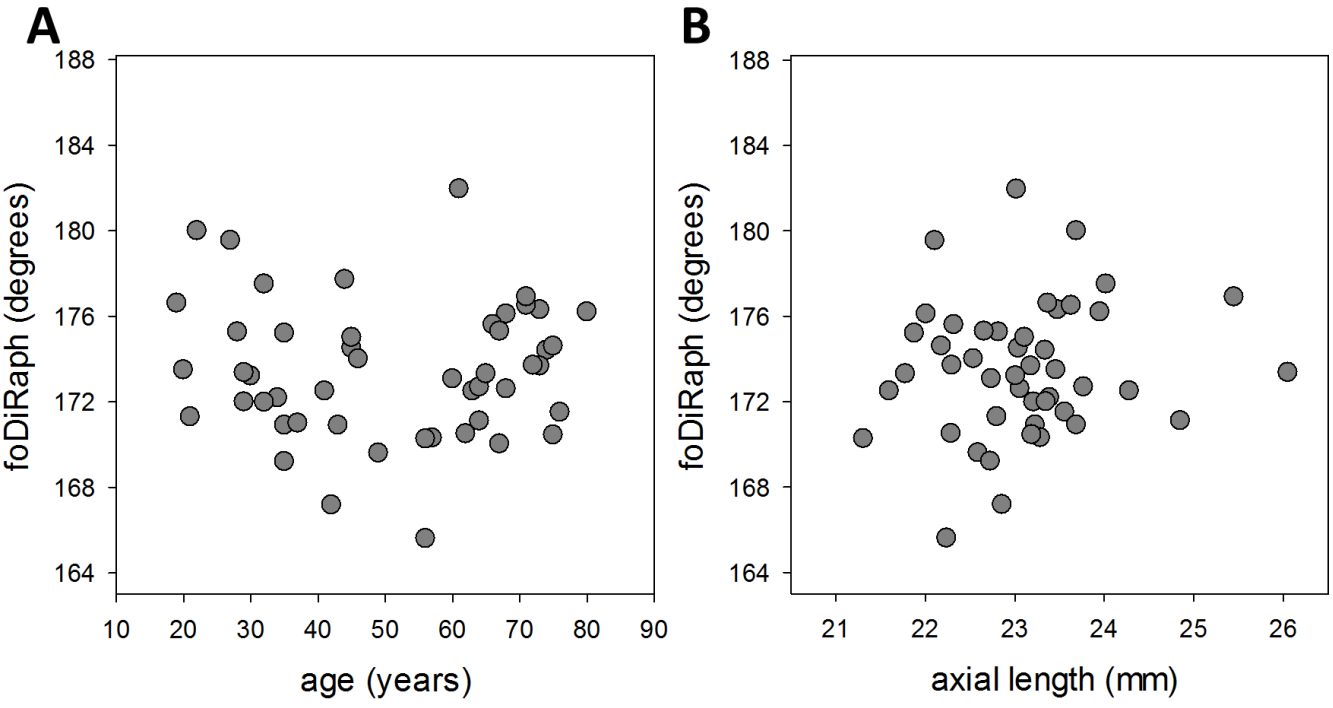

FIGURE 6. Orientation of the temporal raphe in healthy controls as a function of (**A**) age and (**B**) axial length.

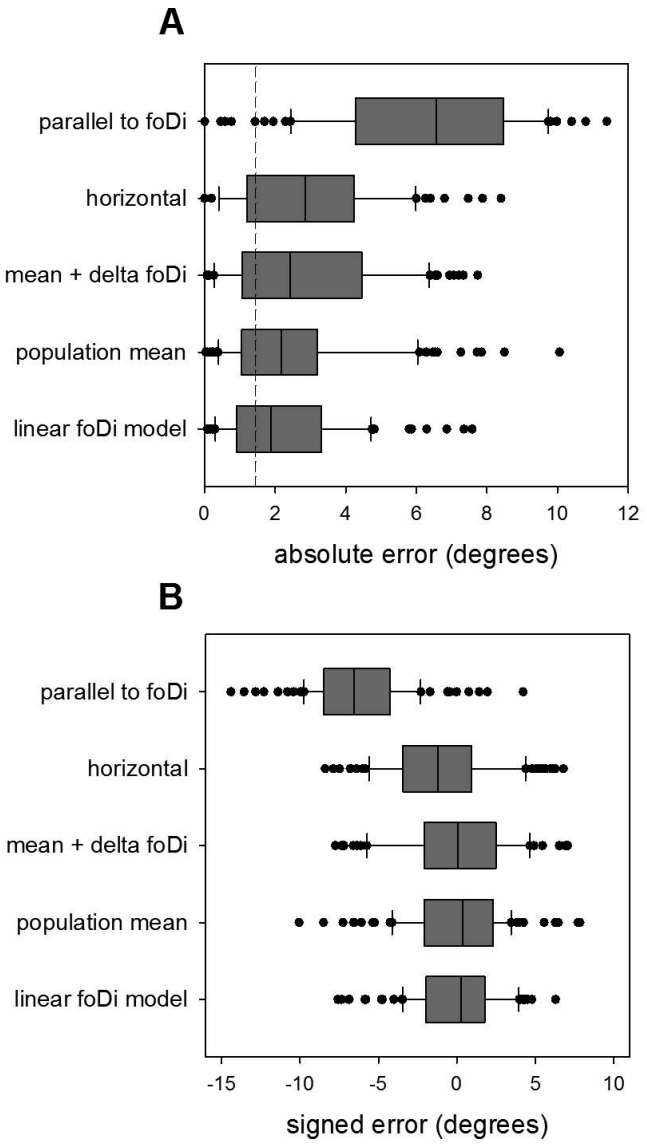

FIGURE 7. Error for estimating orientation of the temporal raphe. Data from healthy controls and patients with glaucoma have been pooled. *Boxes* indicate the interquartile range, and *whiskers* show the 90% range. Outliers are plotted as individual points. From *bottom to top*: application of a linear model fit to the population data, with fovea-disc orientation as the dependent variable; population mean raphe orientation; population mean shifted by an amount equal to the shift of the fovea-disc orientation from its population mean; a horizontal raphe; a raphe aligned with the fovea-disc axis. (**A**) Absolute error, indicating the accuracy of each approximation. The *dashed line* shows direct measurement from macular cube as determined in a previous study on healthy individuals (see text); (**B**) Signed error, revealing bias in some approximations.

absolute error = 6.8°). Assuming a fixed raphe (e.g., horizontal or the population mean) for all subjects was largely equivalent to the assumption of a direct linear relationship between FoDiRaph and FoDi (equations obtained by least squares linear regression were: FoDiRaph = 0.43 × FoDi + 175.7°; FoDiRaph = 0.45 × FoDi + 176.3°, for normal and glaucoma eyes, respectively). This approximation was significantly better than the assumption of a continuation of the fovea-disc axis [$t(96) = -7.0$, $P < 10^{-9}$]. Figure 7B plots the signed error for each approximation, which helps to illustrate that both the fovea-disc and horizontal approximations tend to underestimate the raphe orientation. Both of these approximations gave almost twice as much error (2.5°–2.6°) compared with direct measurement of the raphe from macular cube previously reported for 15 healthy subjects,[14] and these differences were statistically significant to that previous data set [$t(62) = 2.38$, $P = 0.02$ for the horizontal axis and $t(62) = 6.2$, $P < 10^{-7}$ for the continuation of the fovea-disc axis].

It should be noted that although Figure 7 is labeled to describe the error in FoDiRaph, consistent with the terminology preferred in the other figures, the errors reported are actually identical to those for FoRaph. This means that Figure 7 can be used to directly answer the question of how well a horizontal line approximates the raphe itself.

DISCUSSION

This study used a novel algorithm to automatically measure the raphe orientation from intensity information in vertically oriented macular cubes in a population of healthy and glaucomatous eyes. The method is more clinically feasible than the high-density scans typically required to determine the trajectory of the temporal nerve fibers. Substantial variability in the distribution of temporal raphe orientation in both healthy individuals and in patients with glaucoma, with no apparent differences in distribution between groups. In healthy eyes, no correlation was found between raphe orientation and age or axial length of the eye. This study did not specifically aim to include high myopes (only 11/60 participants recruited to the normal group had spherical equivalent refraction less than −1.00 D), so the possibility remains that the raphe may change orientation as a result of myopic stretch. Mild enantiomorphism exists between right and left eyes, despite lack of symmetry in either fovea-disc or fovea-raphe angles. There were no systematic differences in orientation of the raphe, nor in shape parameters of the population distribution, between healthy and glaucoma groups. There did not appear to be any greater uncertainty in localization of the raphe in the glaucoma group.

In regards to conventional assumptions made about the orientation of the temporal nerve fiber raphe, we found that the average raphe is misaligned with the fovea-disc axis by an average of 6.8°, and with the horizontal axis by 3.2°. Individual variation can be large; for example, maximum error was 9.6°. Despite the lesser alignment with the fovea-disc axis, nonetheless the fovea-disc and fovea-raphe angles were correlated, with more superior insertion of the disc tending to "push" the raphe inferiorly.

Since raphe orientation was not accurately predicted by any of the parameters explored (fovea-disc orientation, age, axial length, and symmetry with the contralateral eye), it follows that the raphe orientation should be determined by direct measurement in applications for which the raphe orientation is deemed important. We have recently published an algorithm that can achieve this robustly in clinical populations.[14]

Given recent suggestions that glaucoma is associated with widening of the raphe,[4] it might be expected that progression of the condition would widen the band of minimum intensity across the center of the raphe, hence increasing uncertainty in the determination of raphe orientation. In other words, the accuracy of the method could potentially be reduced in the glaucoma patient population. To determine whether this is the case, the average intensity was calculated for lines traced from the fovea ±5° either side of the raphe center. The distribution of these average line intensities gives a measure of the uncertainty in assigning a fixed raphe orientation. Variance and kurtosis (a measure of peakedness) of this distribution were determined, with no significant difference in either

parameter between the healthy and glaucoma populations [$t(98) = 0.9$, $P = 0.4$ and $t(98) = 0.5$, $P = 0.6$, respectively]. The method therefore suffers no loss in robustness when applied to glaucoma populations, as compared with healthy controls.

There are various applications related to the diagnosis and management of glaucoma for which knowledge of the orientation of the temporal nerve fiber raphe may be considered important. In regards to visual field testing, commonly used indices such as the Glaucoma Hemifield Test[7] and Cluster Analysis[8] inherently presume the relevance of a horizontal axis of symmetry. Analogous comparisons across hemifields are also made on OCT data; for example, the Spectralis software makes comparisons of symmetry in retinal nerve fiber thickness within the macular cube, using the FoDi line as a proxy for raphe orientation.[9]

Beyond such "within platform" metrics, an active area of current research attempts to accurately match visual field data to the corresponding anatomical data in order to improve predictive power. Previous work[17] from our group used a model of axon growth together with ocular biometry data to predict that in 12% of patients, points in the vulnerable nasal step region would be mapped to the opposite pole of the disc from the canonically expected position. That study assumed a population average orientation of the temporal raphe; in light of the variability shown in the present study, even less predictability should be expected for real-world mapping.

In conclusion, there is substantial natural variation in the orientation of the temporal nerve fiber raphe, which cannot be accurately predicted from age, axial length, relative geometry of the disc and fovea, or parameters from the contralateral eye. For applications in which raphe orientation is considered important, it should be measured directly, and it is feasible for this to be incorporated as an automatic feature in modern OCT suites.

Acknowledgments

Supported by Australian Research Council (ARC) Linkage Project LP13100055 and research support from Heidelberg Engineering GmBH, Heidelberg, Germany. The sponsor and funding organization had no role in the design or conduct of this research.

Disclosure: **P. Bedggood**, None; **B. Nguyen**, None; **G. Lakkis**, None; **A. Turpin**, None; **A.M. McKendrick**, None

References

1. Vrabec F. The temporal raphe of the human retina. *Am J Ophthalmol*. 1966;62:926–938.
2. Chauhan BC, Sharpe GP, Hutchison DM. Imaging of the temporal raphe with optical coherence tomography. *Ophthalmology*. 2014;121:2287–2288.
3. Huang G, Gast TJ, Burns SA. In vivo adaptive optics imaging of the temporal raphe and its relationship to the optic disc and fovea in the human retina. *Invest Ophthalmol Vis Sci*. 2014; 55:5952–5961.
4. Huang G, Luo T, Gast TJ, Burns SA, Malinovsky VE, Swanson WH. Imaging glaucomatous damage across the temporal raphe. *Invest Ophthalmol Vis Sci*. 2015;56:3496–3504.
5. Hood DC, Raza AS, de Moraes CGV, Liebmann JM, Ritch R. Glaucomatous damage of the macula. *Prog Retin Eye Res*. 2013;32:1–21.
6. Goldbaum MH, Jang G-J, Bowd C, et al. Patterns of glaucomatous visual field loss in sita fields automatically identified using independent component analysis. *Trans Am Ophthalmol Soc*. 2009;107:136–144.
7. Åsman P, Heijl A. Glaucoma hemifield test: automated visual field evaluation. *Arch Ophthalmol*. 1992;110:812–819.
8. Naghizadeh F, Holló G. Detection of early glaucomatous progression with octopus cluster trend analysis. *J Glaucoma*. 2014;23:269–275.
9. Yamashita T, Sakamoto T, Kakiuchi N, Tanaka M, Kii Y, Nakao K. Posterior pole asymmetry analyses of retinal thickness of upper and lower sectors and their association with peak retinal nerve fiber layer thickness in healthy young eyes. *Invest Ophthalmol Vis Sci*. 2014;55:5673–5678.
10. Garway-Heath DF, Poinoosawmy D, Fitzke FW, Hitchings RA. Mapping the visual field to the optic disc in normal tension glaucoma eyes. *Ophthalmology*. 2000;107:1809–1815.
11. Jansonius NM, Schiefer J, Nevalainen J, Paetzold J, Schiefer U. A mathematical model for describing the retinal nerve fiber bundle trajectories in the human eye: average course, variability, and influence of refraction, optic disc size and optic disc position. *Exper Eye Res*. 2012;105:70–78.
12. Amini N, Nowroozizadeh S, Cirineo N, et al. Influence of the disc–fovea angle on limits of RNFL variability and glaucoma discrimination. *Invest Ophthalmol Vis Sci*. 2014;55:7332–7342.
13. Le PV, Tan O, Chopra V, et al. Regional correlation among ganglion cell complex, nerve fiber layer, and visual field loss in glaucoma. *Invest Ophthalmol Vis Sci*. 2013;54:4287–4295.
14. Bedggood P, Tanabe F, McKendrick AM, Turpin A. Automatic identification of the temporal retinal nerve fiber raphe from macular cube data. *Biomed Opt Exp*. 2016;7:4043–4053.
15. Kim YK, Yoo BW, Kim HC, Park KH. Automated detection of hemifield difference across horizontal raphe on ganglion cell–inner plexiform layer thickness map. *Ophthalmology*. 2015; 122:2252–2260.
16. Denniss J, Turpin A, McKendrick AM. Individualized structure–function mapping for glaucoma: practical constraints on map resolution for clinical and research applications. *Invest Ophthalmol Vis Sci*. 2014;55:1985–1993.
17. McKendrick AM, Denniss J, Wang YX, Jonas JB, Turpin A. The proportion of individuals likely to benefit from customized optic nerve head structure-function mapping. *Ophthalmology*. 2017;124:554–561.

Investigative Ophthalmology & Visual Science